Phonon and elastic instabilities in rocksalt calcium oxide under pressure: a first-principles study

2009 J. Phys.: Condens. Matter 21 015402

(http://iopscience.iop.org/0953-8984/21/1/015402)

J. Phys.: Condens. Matter **21** (2009) 015402 (6pp) doi:10.1088/0953-8984/21/1/015402

Phonon and elastic instabilities in rocksalt calcium oxide under pressure: a first-principles study

Jingyun Zhang and Jer-lai Kuo[1]

School of Physical and Mathematical Sciences, Nanyang Technological University, Singapore 637371, Singapore

E-mail: zhan0184@ntu.edu.sg

Received 24 August 2008, in final form 28 October 2008
Published 2 December 2008
Online at stacks.iop.org/JPhysCM/21/015402

Abstract

The lattice and elastic instabilities of rocksalt (RS) calcium oxide CaO under pressure are extensively studied to reveal the physically driven mechanism of the phase transition from RS to CsCl structure by using the pseudopotential plane-wave method within density-functional theory. The predicted phase transition pressure is 66.38 GPa, employing the total energy method, which falls in the experimental transition pressure range of 60–70 GPa. A pressure-induced soft transverse acoustic (TA) phonon mode is identified at the zone boundary X point in the Brillouin zone, signifying a structural instability. A predicted charge transfer from Ca to O with pressure might be attributable to the phonon softening. Moreover, a softening behavior in the C_{44} shear modulus with pressure is predicted. Analysis of the calculated results suggested that, with increasing pressure, the predicted TA phonon softening behavior, instead of C_{44} shear modulus instability, is mainly responsible for the pressure-induced structural phase transition. We also find that the bond between Ca and O becomes more ionic under compression from Mulliken population analysis.

CaO along with the other members of the alkaline earth oxides family, MgO, BaO and SrO, have long been the focus of geological research since they are important materials of the Earth's lower mantle [1–4]. It is also an important material for a wide range of technological applications, such as in refractory systems, as a reaction facilitator [5] and in plasma displays [6]. Furthermore, they have served in the past as prototypical oxides for testing semi-empirical theories [7]. From the experimental point of view, the behavior under pressure of these solids has been investigated by several authors. In particular, a transition from the rocksalt (RS) (NaCl structure) to the B2 (CsCl structure) phase was detected for CaO at 60–70 GPa by shock wave [1, 8] and diamond anvil cell compression [2, 8]; on the theoretical side, the cohesive energy and structural properties were calculated by Cortonay *et al* [9] through *ab initio* self-consistent calculations and Kalpana *et al* [10] by the linear-muffin-tin-orbitals (LMTO) method. Band-structure calculations have been performed by the linearized-augmented plane-wave (LAPW) [11] and LMTO [12] methods. Results have also been obtained by using the Korringa–Kohn–Rostoker (KKR) method [13]. Lattice dynamical properties were investigated by Schütt *et al* [14] employing the density-functional perturbation theory within the local density approximation at zero pressure. Vibrational properties with pressure and the thermodynamic properties were investigated with the same method mentioned above and the authors assumed that the phase transition from B1 to B2 may due to the phonon instability. Very recently, the effects of pressure on the elastic constants were studied by Louail *et al* [15] and Deng *et al* [16] who attribute the phase transition from B1 to B2 to the elastic instability using the plane-wave pseudopotential method. So until now there still exists controversy about the physically driven mechanism of the phase transition occurring in CaO. The present paper aims at a systematic study to probe the transition mechanism and achieve a conclusive result. Dynamical [17] and elastic instabilities [18] are often responsible for phase transitions under pressure. Detailed *ab initio* calculations of the lattice dynamics and elastic constants for CaO are, thus, motivated.

Pseudopotential plane-wave *ab initio* calculations were performed within the framework of density-functional

[1] Author to whom any correspondence should be addressed.

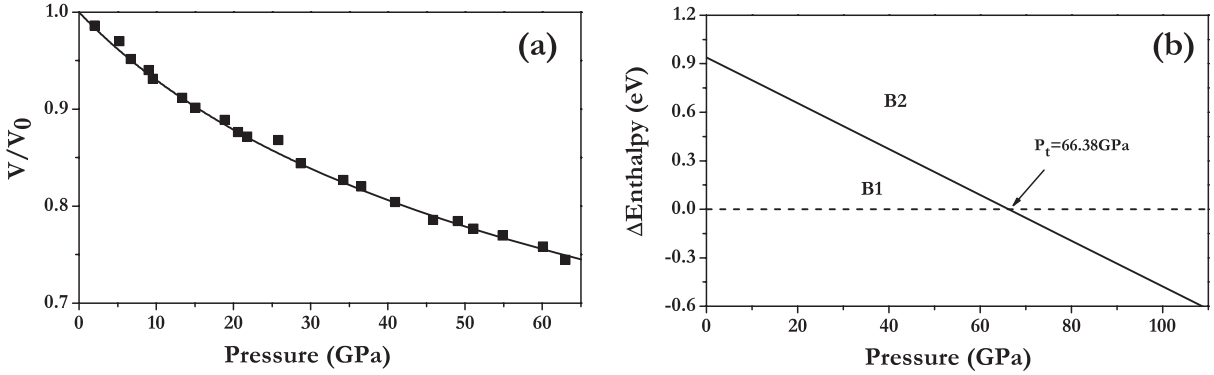

Figure 1. Comparison of the calculated equation of states (solid line) for CaO with the experimental data (solid square symbols) from [2] are shown in the left panel (a). The right panel (b) displays the enthalpy difference of the B1 and B2 structures.

theory [19]. The generalized gradient approximation (GGA) exchange–correlation functional [20] was employed. The norm-conserving scheme is used to generate the pseudopotentials for Ca and O. The core radii for Ca and O are chosen to be sufficiently small to guarantee the core non-overlapping under compression in this study. Convergence tests gave a kinetic energy cutoff, E_{cutoff}, as 70 Ryd and a $8 \times 8 \times 8$ Monkhorst–Pack (MP) [21] grid (k-mesh) for the electronic BZ integration. The lattice dynamics of these compounds were investigated by using the linear-response method [22]. A $12 \times 12 \times 12$ MP k-mesh was found to yield phonon frequencies converged to within 0.05 THz. A $4 \times 4 \times 4$ q mesh in the first BZ was used in the interpolation of the force constants for the phonon dispersion curve calculations. All the properties mentioned above are calculated by the QUANTUM-ESPRESSO package [23]. A technique for the projection of plane-wave states onto a localized basis set is used to calculate atomic charges and bond populations by means of Mulliken analysis as implemented in CASTEP [24]. The elastic constant tensors were calculated as a function of pressure using the stress–strain relations. Elastic constants were obtained from evaluations of the stress tensor generated by small strains using the density-functional plane-wave technique.

The theoretical equilibrium lattice constant is determined by fitting the total energy as a function of volume to the Murnaghan equation of states (EOS) [25]. The calculated equilibrium lattice parameters and bulk modulus, together with other theoretical calculations [16, 26–29] and the experimental data [4, 30], are listed in table 1. Table 1 lists the calculated elastic constants for CaO, together with experimental data [37, 38] and previous theoretical results [16, 26–29] at ambient pressure. It is clear that the current theoretical lattice constants and bulk modulus are in good agreement with experimental data within 0.5%. The excellent agreement strongly supports the choice of pseudopotentials and the GGA approximation for the current study. The calculated EOS of CaO in the RS structure is compared with the experimental data [2] as shown in figure 1(a). The agreement between theoretical results and the experimental data is also satisfactory, lending another support to the validity of the current theoretical model, especially guaranteeing the accuracy of the high pressure study. We can

Table 1. Calculated equilibrium lattice parameter (a_0), bulk modulus (B_0) and elastic constants of C_{11}, C_{12}, C_s and C_{44} for CaO. Previous theoretical calculations and experimental results are also shown for comparison. The units for a_0 and B_0 are in Å and GPa, respectively.

		a_0	B_0	C_{11}	C_{12}	C_{44}
B1	Our work	4.834	109.679	207.400	58.300	75.950
	Ref. [25]	4.720	128.000	274.000	54.000	53.000
	Ref. [26]	4.820	102.000	206.000	50.000	66.000
	Ref. [27]	4.838	117.000	239.000	51.600	77.400
	Ref. [28]	4.840	109.000	223.000	53.000	84.000
	Ref. [16]	4.810	111.990	215.13	66.940	77.820
	Ref. [29]	4.714	129.000			
	Exp. 4	4.811	110.000			
	Exp. 36			221.890	57.810	80.320
	Exp. 37			220.530	57.670	80.030

estimate the transition pressure from the usual condition of equal enthalpies, i.e. the pressure P, at which the enthalpies, $H = E + PV$, of both the B1 and B2 structures is the same. The enthalpy H as a function of pressure P is illustrated in figure 1(b), the enthalpy of B1 taken as reference. It is found that the phase transition from the B1 phase to the B2 phase of CaO occurs at 66.38 GPa, within the experimental range of 60–70 GPa [1, 2].

We have calculated the complete phonon dispersion curves for CaO with increasing pressure and projected phonon density (PPDOS) of states which was shown in figure 2. Panel (a) of figure 2 shows the comparison of the calculated phonon dispersion curves with the experimental data (solid squares) [31] at ambient conditions. With the addition of the nonanalytic term to the dynamical matrix, the longitudinal optic (LO) phonon branch and the transverse optic (TO) phonon branch split from each other at the Γ point, and this is shown. It is clear that the calculated phonons successfully reproduced the experimental data at all high symmetry directions in the BZ. The right panels in figure 2 show the calculated PPDOS. It is important to note that the O atom mainly contributes to the high frequency vibrations because of its relatively lighter atomic mass, while the Ca atom dominates the low frequency vibrations as expected. We found that, at the theoretical equilibrium volume of the RS structure, all phonon modes are stable. It is interesting to note

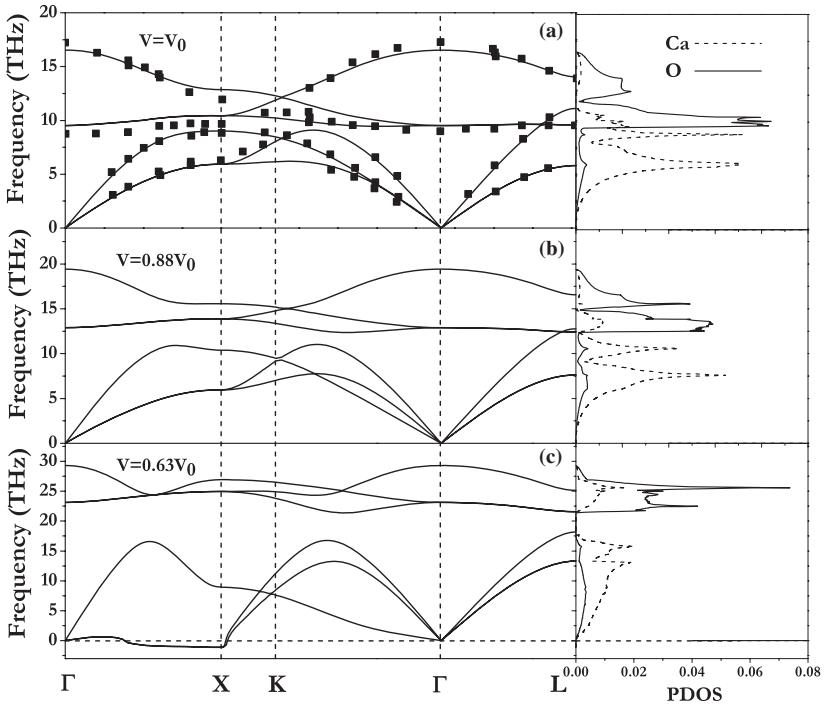

Figure 2. The calculated phonon dispersion curves of CaO at different volumes. Solid squares are the experimental data taken from [30].

that, with decreasing volume, the TO, LO and longitudinal acoustic (LA) phonon modes shift to higher frequencies, while the transverse acoustic (TA) phonon branch along the [100] direction decreases in frequency, indicating a negative mode Grüneisen parameter, $\gamma_j(q) = -\partial \ln \nu_j(q)/\partial \ln V$ for mode j, where q is the wavevector, ν is frequency and V is the volume. It is significant that, with an increase in pressure, the TA phonon frequency at the zone boundary X (0.0 0.0 1.0) point softens to imaginary frequencies at $V = 0.63V_0$ (V_0 is the theoretical equilibrium volume), indicating a structural instability. The TA(X) mode Grüneisen parameter under compression was depicted in figure 4(d). As can be seen from the figure, the Grüneisen parameter ranges mostly from 0 to -20 and all are negative, which suggests that the frequency of TA(X) decreases with increasing pressure. Figure 3 shows the variation of the squared frequency of the TA(X) mode with pressure. The estimated pressure of phonon softening to zero frequency is 158 GPa, which is somewhat larger than the experimental transition pressure of 60–70 GPa. A near-perfect linear relation between ν^2 and pressure was obtained. Such behavior is consistent with the Landau theory of pressure-induced soft mode phase transitions [32].

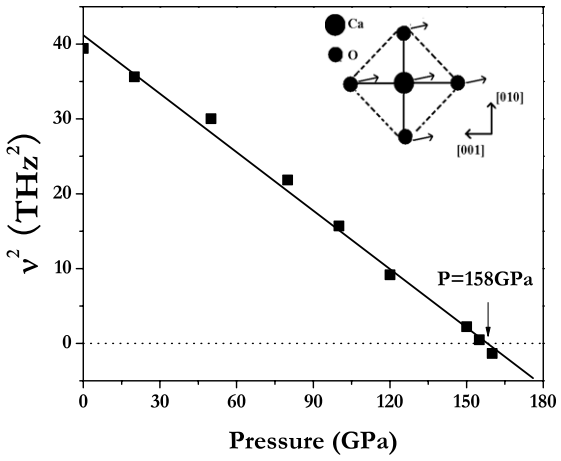

Figure 3. The calculated TA(X) phonon frequencies in CaO as a function of pressure. The solid line through the calculated data is a linear fitted curve. The eigenvector for TA soft phonon mode is at the X (1.0 0.0 0.0) point for CaO. The Ca atom is located at (0, 0, 0). The other four O atoms sit at (0, 1/2, 0), (0, −1/2, 0), (0, 0, 1/2) and (0, 0, −1/2), respectively. The arrows show the directions of atomic displacements.

In general, the predicted TA(X) phonon softening in CaO shed a strong light on the physical mechanism behind the phase transition. The somewhat large difference in transition pressures between theory and experiment indicates that the phase transition from the RS to CsCl structure might not be induced independently by the dynamic instability. However, although the phase transition occurs at pressures below those required to drive TA(X) modes to zero frequency, the 'mode softening' behavior may be related to the particular mechanisms which are responsible for the phase transition. The RS CaO, therefore, tends to become unstable with respect to the atomic displacement corresponding to the soft mode. Inspection of the phonon eigenvector shows that this mode involves alternate shuffles of (100) planes. Interestingly, the eigenvector of this soft mode for both Ca atoms and O atoms is shown in the inset of figure 3. The atomic movements along the directions of the eigenvectors in the (100) planes are closely related to the phase transition from RS to CsCl structure.

For an insulator, the Born effective charge is a measure of the change in electronic polarization due to ionic displacements. The form of effective charge tensor for the

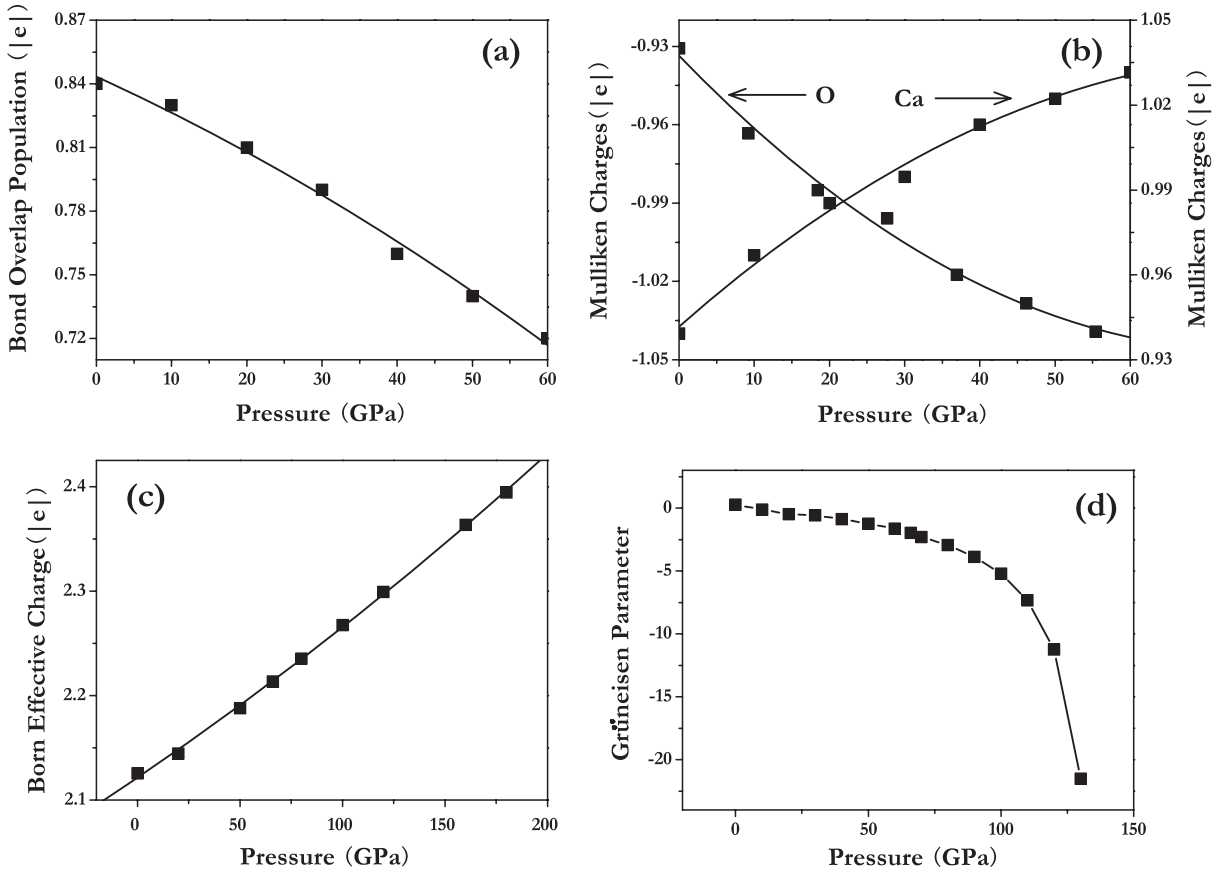

Figure 4. (a) and (b) are the calculated bond overlap population and Mulliken charges for CaO with pressure, respectively; (c) the calculated Born effective charge for Ca as a function of pressure; (d) the calculated Grüneisen parameter for TA(X) mode with pressure. The symbols are the calculated data and the lines are guides for the eye. In (b), the left scale is for O, while the right scale is for Ca.

constituents is determined by the site symmetry of the ions. In CaO, the Ca ion occupies the 4a Wyckoff position. Therefore, one would expect its effective charge tensor to be isotropic. The most important conclusion from figure 4(c) is that the Born effective charges for Ca increase with pressure in the pressure range considered. Pressure-induced increase of the effective charge indicates a charge redistribution.

To further demonstrate the bonding behavior of CaO, we use Mulliken population analysis [33] to explore the bond overlap population (BOP) and Mulliken effective charge as shown in figure 4. It was found that the spilling parameters in this calculation were very low at 10^{-3}, indicating a good representation of the electronic bands using the linear combination of atomic orbitals basis set. A spilling parameter in the region of 10^{-3} indicates that only approximately 0.1% of the valence charge has been missed in the projection [34]. The BOP was widely used to assess the covalent or ionic bonding nature of particular bulk crystals. A high value of the BOP indicates a high degree of covalency in the bond, while a low value indicates a more ionic interaction. With increasing pressure, the BOP of CaO was reduced from $0.84|e|$ at zero pressure to $0.72|e|$ at 60 GPa as shown in figure 4(a), indicating a more ionic bonding feature under high pressure and a pressure-induced charge transfer from Ca to O. It is widely accepted that the absolute magnitude of the atomic charges have little physical meaning. However, we demonstrate that consideration of relative values of Mulliken populations, in contrast to the absolute magnitudes, can yield useful information. The variations of Mulliken charges with pressure for Ca and O are explicitly shown in figure 4. Table 2 also lists the effective ionic valences for each of the crystals. This is defined to be the difference between the formal ionic

Table 2. Mulliken overlap populations calculated from plane wavefunction pseudopotential calculations.

Pressure (GPa)	Species	s	p	d	Ionic charge ($\|e\|$)	Effective valence ($\|e\|$)
0	Ca	2.24	6.00	0.73	1.04	0.96
	O	1.89	5.15	0.00	−1.04	3.04
10	Ca	2.22	6.00	0.77	1.01	0.99
	O	1.88	5.14	0.00	−1.01	3.01
20	Ca	2.21	5.99	0.80	0.99	1.01
	O	1.87	5.13	0.00	−0.99	2.99
30	Ca	2.20	5.99	0.83	0.98	1.02
	O	1.86	5.11	0.00	−0.98	2.98
40	Ca	2.19	5.99	0.85	0.96	1.04
	O	1.86	5.11	0.00	−0.96	2.96
50	Ca	2.18	5.99	0.88	0.95	1.05
	O	1.85	5.10	0.00	−0.95	2.95
60	Ca	2.17	5.99	0.90	0.94	1.06
	O	1.85	5.09	0.00	−0.94	2.94

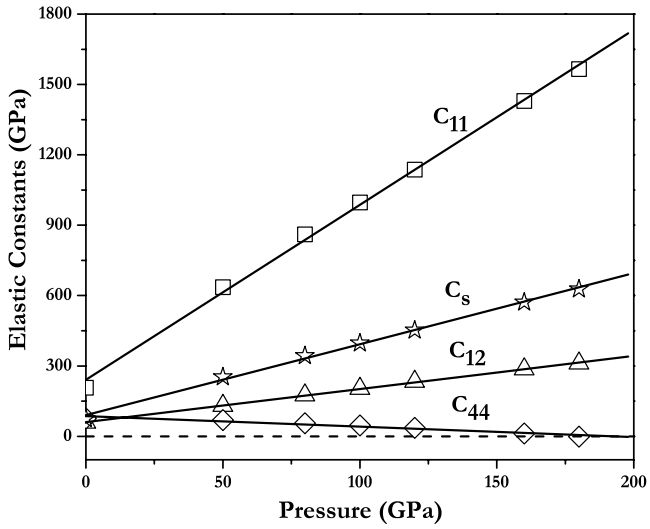

Figure 5. Calculated elastic constants (open symbols) of C_{11}, C_{12}, C_s and C_{44} for CaO with pressure in the RS structure. The solid lines are linear fits to the calculated results.

charge and the Mulliken charge on the anion species in the crystal. This is also used as a measure of iconicity: a value of zero implies an ideal ionic bond while values greater than zero indicate increasing levels of covalency. A pressure-induced charge transfer from Ca to O is clearly revealed to support the validity of the BOP calculation. It is also interesting to note that the CaO become more ionic under high pressure. The predicted charge transfer might significantly alter the competing attractive and repulsive forces between the nearest neighbors, thereby possibly inducing a soft phonon mode [35]. As mentioned above from the right panel of figure 2, the softening TA phonon mode is dominated by the vibration of Ca atoms. This charge-depletion-induced phonon softening is similar to that in the B-doped diamond in which C → B charge transfers drive a Raman redshift [36].

Table 1 lists the calculated elastic constants for CaO, together with experimental data [37, 38] and previous theoretical results [16, 26–29] at ambient pressure, which good agreement was achieved compared with the experimental data and previous theoretical calculations. The variations of the elastic constants with pressure for CaO are shown in figure 5. It is clear that C_{11}, C_{12} and C_s exhibit linearly increasing trends with pressure while C_{44} shows a linear softening trend. It is noteworthy that, although C_{44} softens with pressure for CaO, it still remains positive under pressures at which the phonons soften to zero frequency. It should also be pointed out the phonon instabilities occur at points away from the center of the BZ and appear before the materials become unstable according to elastic stability criteria. Therefore, it is concluded that the pressure-induced structural phase transition for CaO is not dominated by the C_{44} instabilities which are related to the long-wavelength part of the transverse branch near the center of the first BZ.

In this work, we have extensively studied the lattice dynamics and elastic constants of RS CaO under pressure using the *ab initio* pseudopotential plane-wave method. We predicted a pressure-induced soft TA phonon mode at the zone boundary X point. Moreover, a softening behavior in C_{44} shear modulus with pressure is verified for CaO. Analysis of the calculated results suggested that, with increasing pressure, the predicted TA phonon softening behavior, instead of C_{44} shear modulus instability, is closely related to the pressure-induced structural phase transition from RS to CsCl.

Acknowledgments

This work was supported in part under URC grants RG34/05, RG35/05, RG57/05 and RG170/06 from Nanyang Technological University. Computational resources, in part provided by the Computational Chemistry Lab at Nanyang Technological University, are greatly appreciated.

References

[1] Jeanloz R and Ahrens T J 1980 *Geophys. J. Astron. S.* **62** 505
[2] Mammone J F, Mao H K and Bell P M 1981 *Geophys. Res. Lett.* **8** 140
[3] Karki B B, Wentzcovitch R M, de Gironcoli S and Baroni S 1999 *Science* **286** 1705
[4] Richet P, Mao H K and Bell P M 1988 *J. Geophys. Res.* **93** 15279
[5] Choudhary V R, Rajput A M and Mamman A S 1988 *J. Catal.* **178** 576
[6] Cho J H, Kim R, Lee K W, Yeom G Y, Kim J Y and Park J W 1999 *Thin Solid Films* **350** 173
[7] Aguado A, Bernasconi L and Madden P A 2003 *J. Chem. Phys.* **118** 5704
[8] Jeanloz R, Ahrens T J, Mao H K and Bell P M 1979 *Science* **206** 829
[9] Cortonay P and Monteleone A V 1996 *J. Phys.: Condens. Matter* **8** 8983
[10] Kalpana G, Palanivel B and Rajagopalan M 1995 *Phys. Rev.* B **52** 4
[11] Stepanyuk V S, Sz'asz A, Grigorenko A A, Katsnelson A A, Farberovich O V, Mikhalin V V and Hendry A 1992 *Phys. Status Solidi* b **173** 633
[12] Springborg M and Taurian O E 1986 *J. Phys. C: Solid State Phys.* **19** 6347
[13] Yamashita J and Asano S 1983 *J. Phys. Soc. Japan* **52** 3506
[14] Schütt O, Pavone P, Windl W, Karch K and Strauch D 1994 *Phys. Rev.* B **50** 3746
[15] Louail L, Krachni O, Bouguerra A and Ali Sahraoui F 2006 *Mater. Lett.* **60** 3153
[16] Deng Y, Jia O H, Chen X R and Zhu J 2006 *Physica* B **392** 229
[17] Baroni S, de Gironcoli S, Corso A and Giannozzi P 2001 *Rev. Mod. Phys.* **73** 515
[18] Einarsdotter K, Sadigh B, Grimvall G and Ozoliņš V 1997 *Phys. Rev. Lett.* **79** 2073
[19] Baroni S, Giannozzi P and Testa A 1987 *Phys. Rev. Lett.* **58** 1861
[20] Perdew J P and Burke K 1996 *Int. J. Quantum Chem.* **57** 309
Perdew J P, Burke K and Ernzerhof M 1996 *Phys. Rev. Lett.* **77** 3865
[21] Monkhorst H J and Pack J D 1976 *Phys. Rev.* B **13** 5188
[22] Giannozzi P, de Gironcoli S, Pavone P and Baroni S 1991 *Phys. Rev.* B **43** 7231
[23] Baroni S, Dal Corso A, de Gironcoli S, Giannozzi P, Cavazzoni C, Ballabio G, Scandolo S, Chiarotti G, Focher P, Pasquarello A, Laasonen K, Trave A, Car R, Marzari N and Kokalj A http://www.pwscf.org

[24] Segall M D, Lindan P L D, Probert M J, Pickard C J, Hasnip P J, Clark S J and Payne M C 2002 *J. Phys.: Condens. Matter* **14** 2717
[25] Murnaghan F D 1944 *Proc. Natl Acad. Sci. USA* **30** 244
[26] Baltachea H, Khenataa R, Sahnounb M, Driza M, Abbarc B and Bouhafsc B 2004 *Physica* B **344** 334
[27] Mehl M J, Hemley R J and Boyer L L 1986 *Phys. Rev.* B **33** 8685
[28] Karki B B and Crain J 1998 *J. Geophys. Res.* **103** 12405
[29] Tsuchiya T and Kawamura K 2001 *J. Chem. Phys.* **114** 10086
[30] Mehl M J, Cohen R E and Krakauer H 1988 *J. Geophys. Res.* **93** 800
[31] Rieder K H, Weinstein B A, Cardona M and Bilz H 1973 *Phys. Rev.* B **8** 4780
[32] Samara G A and Peercy P S 1981 *Solid State Physics* vol 36, ed H Ehrenreich, F Seitz and D Turnbull (New York: Academic)
[33] Mulliken R S 1955 *J. Chem. Phys.* **23** 1833
[34] Segall M D, Shah R, Pickard C J and Payne M C 1996 *Phys. Rev.* B **54** 16317
[35] Ozolinš V and Zunger A 1999 *Phys. Rev. Lett.* **82** 767
[36] Ekimov E A, Sidorov V A, Bauer E D, Mel'nik N N, Curro N J, Thompson J D and Stishov S M 2004 *Nature* **428** 542
[37] Chang Z P and Graham E K 1977 *J. Phys. Chem. Solids* **38** 1355
[38] Oda H, Anderson O L, Isaak D G and Suzuki I 1992 *Phys. Chem. Miner.* **19** 96105